STRUCTURE AND MINERALOGY OF THE MURO ALTO GRANITIC PEGMATITE (VIEIRA DO MINHO - PORTUGAL) – PECULIAR ASSEMBLAGES OF HIGH-F HYDROTHERMAL EVOLUTION

Dias, P. A.[1]
Pereira. B.[2]
Leal Gomes. C.[1]
Guimarães, F.[3]

[1] Universidade do Minho – CIG-R - Escola de Ciências- Gualtar-4710-057 BRAGA, Portugal
[2] Sinergeo LDA. Edifício IEMINHO Lugar de Casal 4730-575 Soutelo - VILA VERDE
[3] LNEG- Rua da Amieira,4465, S. MAMEDE DE INFESTA

Keywords: coupled LCT pegmatites; hydrothermal evolution; hydraulic breccia.

INTRODUCTION

In the place of Muro Alto, in Vieira do Minho, until the 1970s, two contiguous and spatially related pegmatites (hereinafter referred to as W and E bodies) were mined for Ta, Nb, Be, and Sn. Both pegmatites show LCT specialization (Li, Cs, Ta) and are hosted in a syntectonic granite of the 3rd phase of Variscan deformation (D3) (Fig. 1). However they exhibit sensitive differences in composition: the W body has abundant beryl and Al-Li phosphates; the E body is paragenetically more evolved with abundant lepidolite. The study of the structure and paragenesis of the Muro Alto pegmatites suggests the existence of typical correlations between the original F/OH ratio in successive fluid-magmatic differentiates and protracted late hydrothermal evolution in this genetically interrelated pegmatitic pair. As a hypothesis, the same volatile ratio may have been responsible for increasing paragenetic diversification of phosphates, Nb-tantalates, and micas mineralogical groups.

Methodologically the discrimination of minerals (Table 1) used X-ray diffraction analysis and microtextural analysis in reflected light and electron microprobe (EPMA). Compositions of minerals and its variability were determined in electron microprobe.

Table 1. Mineralogical associations assigned to the internal structure of the pegmatites, highlighting the most differentiating characters.

Internal Units	*W pegmatite - Larger open pit*	*E pegmatite – Smaller open-pit*
Border unit	Consists of quartz, feldspars, botryoidal muscovite	Consists of quartz, feldspars, lithian botryoidal muscovite, black mica, tourmaline (schorl).
Intermediate zone	Essentially feldspathic with lithian radial muscovite or in bands (layer).	Essentially orthosis with later lepidolite generation
Core	Consisting of quartz and "comb-structure." beryl	Mainly quartz with sparse potassium feldspar crystals and F-elbaite aggregates.
Late units	Albitic with subsidiary microcline	Lepidolitic and albitic with Li-Cs-mica.
Typomorphic accessory phases	Amblygonite-montebrasite (and phosphate products of hydrothermal alteration), rare spodumene altered to coockeite and smectite, beryl (yellow), bertrandite, Fe-columbite - tantalite-Fe, gahnite, uranomicrolite (pyrochlore).	F-elbaites, blue beryl, cassiterite, topaz, fenacite, Cs-lepidolite, Mn-columbite - Mn-tantalite, pseudostaringite, uranomicrolite.
Metalogenic specialization	LCT>>NYF: Nb>Ta>W, U>T.R.-Y, Be>Li, F>B; W	LCT most marked: Ta□Nb>Sn, F=B, Be□Li
Other aspects	Larger, deeper location (possible more proximal to the residual granitic magma source).	Smaller, aplitic wall unit (similar to a "line-rock"). There is a boron-lithium breccia with microcline clasts suggesting the manifestation of culminating episodes of high internal tension steam.

PECULIAR TEXTURES

There are some textures, habits and aggregates, that are sporadic in other pegmatites but are typical here:

1 – beryl megacrysts (yellow variety) may be involved in botryoidal aggregates of mica in the intermediate zone of the W pegmatite (sceptre texture, Fig. 1);

2 – mica in bands is also common;

3 - late zircon in druses is nucleated in the intercrystalline space between beryl and the sceptre mica;

4 - lamellar Nb-tantalates intergrown with different major minerals - white mica, feldspar, and lilac lepidolite - include columbites - tantalites, uranomicrolites, which may be associated with cassiterite; some lamellar columbites -

tantalites intergrown with mica, show radial texture (Fig. 1);

5 - coarse phosphate crystals, especially amblygonite-montebrasite and products of hydrothermal evolution, occur in the transition to the quartz core; late fibrous montebrasite intergrown with white mica, may represent a pseudomorphic evolution in subsolidus of primitive megacrysts (possible spodumene);

6 - pink botryoidal mica in the intermediate zone of the E pegmatite occur nucleated in sceptre on dark mica lamellae;

7 – hydrothermal breccia with angular potassium feldspar clasts (microclinized and reddened); the matrix cement is composed of green tourmaline and white-pink micaceous aggregates.

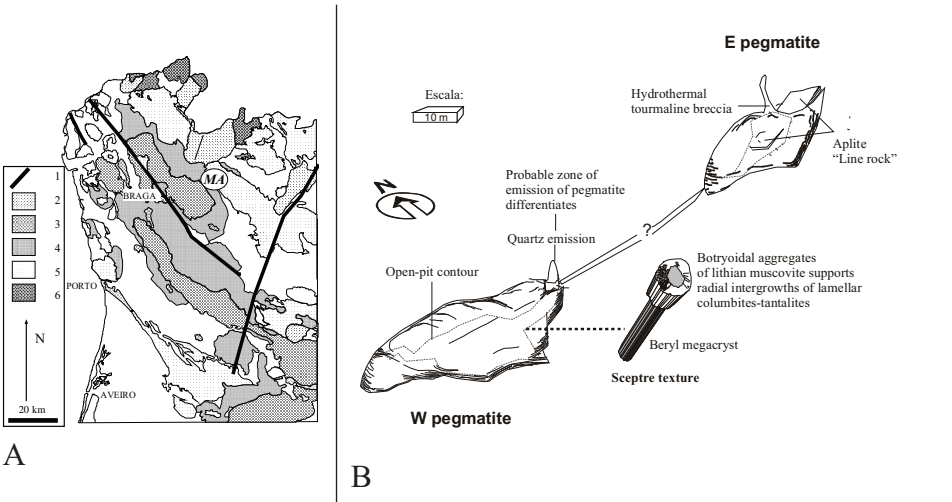

Figure 1- A) Location of Muro Alto (MA). Symbols: 1- major tectonic lineaments; 2 – Post- tectonic granites in relation to D3 Variscan folding phase; 3 - D3 late tectonic granitoids related with ductile shear; 4 - D3 sin-tectonic granitoids related with ductile shear; 5 – two mica granites sin - tectonic in relation to D3; 6 – restitic two mica granites and migmatites. B) Three-dimensional structural relationships of the Muro Alto cogenetic pair of pegmatites – 3D simulated forms. The geometry is indicated by beryl - mica - lamellar niobium-tantalates.

PARAGENESES AND MINERAL CHEMISTRY

Examples of intergrowths between Nb and Ta minerals and their more conspicuous zoning patterns are illustrated in Figure 2. The Nb-tantalates intergrown with mica from the W open-pit have convolute epitaxic overgrowth with oscillatory zoning, which can be attributed to the destabilization of the primitive Fe-columbite. The evolutionary trend expresses similar Nb and Ta contents, but is enriched in Fe relative to Mn. The highest WO_3 content (up to 5%) occur in the later and Fe richer Nb-tantalates. The oscillatory zoning and the primary phases are truncated by uranomicrolite venules (Table 2).

In the E pegmatite, Mn enrichment is observed that is typical of most LCT

pegmatites, but the evolution culminates in Mn-columbite crystallization. The paragenesis also includes Nb-tantalates with high Sn content (Table 2). The observed intergrowths show exsolution from cassiterite and phases that could tend to a "pseudo-staringitic" composition (with up to 6.13% of Ta_2O_5, Table 2) (compare with Beurlen et al. 2003). The projections are in the reference line: 3 $(Ti, Sn)^{4+}$ = $(Fe, Mn)^{2+}$ 2 $(Nb, Ta)^{5+}$ and diverge from the $(Ta^{5+}, Nb^{5+}) = 2.00$ reference line.

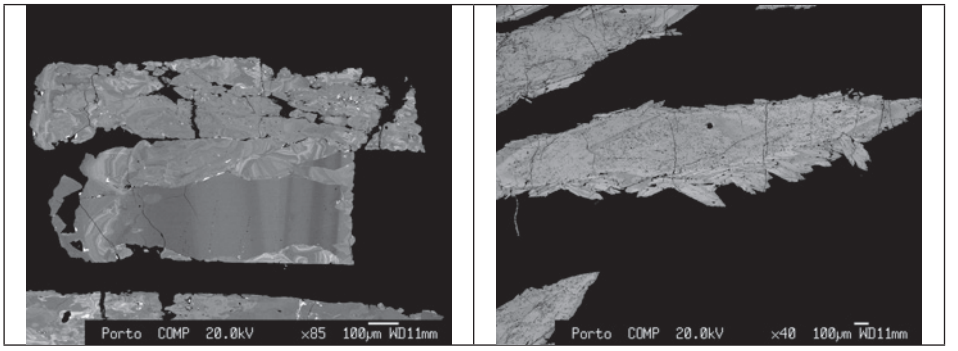

Figure 2 - Patterns of truncated oscillatory zoning, and epitaxic overgrowths in sections of Nb-Ta-Sn oxides.

Table 2. EPMA of selected compositions of Sn-Nb-Ta oxides.

	cassiterite	pseudo-staringite	cassiterite wodginite	Mn-columbite	U-microlite	Fe-columbite				Fe-tantalite		Fe-columbite epitáxica	Fe-columbite percursora
	1	2	3	4	5	6	7	8	9	10	11	12	13
FeO	0,27	0,27	2,02	1,06	0,05	13,17	10,90	10,60	10,73	9,51	9,36	10,86	14,9
TiO_2	0,46	-	0,04	0,82	0,21	0,22	0,39	1,72	1,34	0,19	0,24	1,99	1,97
MnO	-	0,66	6,49	18,08	0,00	4,79	8,15	7,58	7,36	5,73	6,23	8,42	3,69
SnO_2	98,45	91,89	47,67	0,10	0,34	0,17	0,07	0,29	0,25	1,07	0,51	0,20	-
WO_3	-	-	0,33	2,97	0,69	-	1,38	3,80	4,11	2,53	2,61	3,91	4,76
Ta_2O_5	0,30	6,13	35,15	20,60	68,33	44,93	37,77	24,58	34,45	58,90	55,10	14,11	17,16
Nb_2O_5	1,02	1,40	7,32	53,99	1,69	35,71	40,10	50,71	42,55	21,36	25,09	57,66	57,54
MgO	-	-	-	-	-	0,23	0,17	-	-	-	-	-	-
UO_2	-	-	-	-	11,04	0,05	-	-	-	-	-	0,10	-
Sc_2O_3	-	-	-	-	0,66	0,41	0,22	0,09	0,13	0,24	0,18	0,11	0,05
ZrO_2	-	-	-	-	0,37	-	0,81	0,81	0,18	1,21	0,69	0,61	0,16
Na_2O	-	-	-	-	5,00	nd	nd	-	0,02	-	0,06	-	-
CaO	-	-	-	-	5,27	nd	nd	-	-	-	-	-	-
Sb_2O_5	-	-	-	-		0,27	0,12	-	-	-	-	-	-
Total	100,49	100,35	99,02	97,61	93,65	99,93	100,07	100,23	101,11	100,75	100,08	98,06	100,3

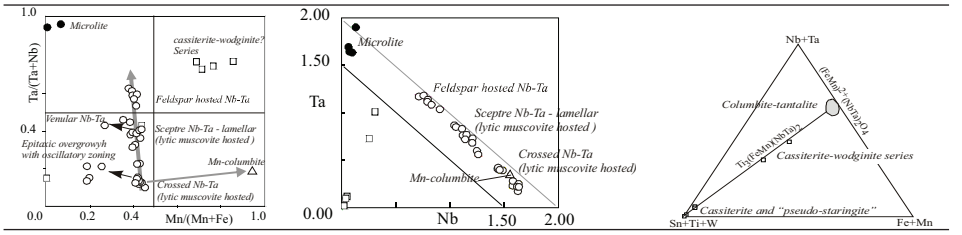

Figure 3 - Trends of mineral-chemical fractionation of Nb-tantalates and cassiterite.

The mineral-chemistry of Nb and Ta oxides suggests the main fractionation – Fe-columbite => Fe-tantalite => uranomicrolite in the W pegmatite and Mn-columbite => cassiterite-wodginite series => uranomicrolite in the E pegmatite, attributable to a magmatic - hydrothermal transition possibly accompanied by increasing F mineralogic sequester.

U-rich zircon is common in the vicinity of the Nb-tantalates, sometimes with a P-rich phase (P_2O_5 <12.1%) and also with F. The first is paragenetically concurrent with U-microlite. The P-rich zircon is posterior and may be related to the late evolution of phosphates. The zircon intergrown with lepidolite in the E body has high Hf content (6.84-8.91%). This behaviour is typical of the normal evolution of evolved LCT pegmatites.

X-ray diffraction applied to the study of phosphates identifies amblygonite as the primary predominant phosphate. Electron microprobe chemical analysis show very high F content (± 9%) and indicate the substitutions expressed in the formula, (Li, Na) $AlPO_4$ (OH, F). Coexistence with other F-rich minerals (such as topaz) suggests that the evolutionary culmination in the magmatic-hydrothermal transition is marked by F enrichment. In some petrogenetic modelling, hydrothermal evolution above 400°C increases the diversity of phosphates, easing the transition between crystal structures. The later crystal-chemical readjustments preserve the high F signature, which is manifested in the Mn/Fe relations (childrenite-eosphorite with F up to 0.65%) or the increase of Ca (crandallite with F between 1.18 and 2.09%). Baldwin et al. (2000) suggested temperatures of 300-200°C for the deposition of crandallite). The formation of morinite (with 15% of F) may be one of the last products of the rebalancing of phosphates. Its precipitation and also of a late triplite-zwiselite (with 6.5% of F) must have occurred at temperatures below the crandallite. Some gahnites - ($Zn_{0.62}$, $Fe_{0.46}$, $Mn_{0.01}$) ($Al_{1.6}$, $Fe_{0.4}$) O_4 - occasionally corroded, are included in amblygonite and may represent the initial magmatic stage.

In the matrix of the feldspathic breccia in the E pegmatite, green tourmalines occur and are identified as F-elbaites. The electron microprobe analysis shows that the compositional variation between the core and rim is explained by the substitution $2Fe^{2+}$ (Y) ⇔Li (Y) + Al (Y) - Li richest core and Fe poorest. The reverse change occurs in the coexisting micas. The core – rim transition is made towards the Li-rich mixed forms, which unlike the other Li-micas, have significant Fe content.

In Figure 4 diagrams, primary micas of the intermediate zone of the W pegmatite and botryoidal micas of the marginal zone of the E pegmatite, lie along the same fractionation trajectories. With the exception of Fe that may have oscillatory behaviour, the pegmatitic fractionation shows Li and Rb enrichment. In the E body, the Li + Cs metasomatism - Cs^+ / Cs^+/Li^+ e (Cs^+, Li^+)/(Na^+, K^+) substitutions - leads to Cs-rich lepidolites, pseudomorphic or originated by direct deposition.

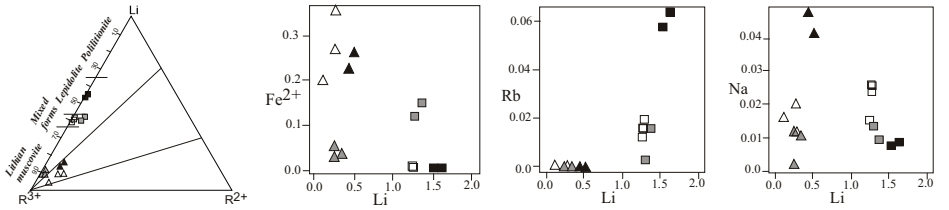

Figure 4 - Projections in apfu of micas from different paragenetic situations. Open triangle -botryoidal muscovite (intermediate zone, W pegmatite); black filled triangle - botryoidal light pink muscovite (board, E pegmatite); grey filled triangle and grey square – zoned lithian muscovites and lepidolites of the hydrothermal breccia (E pegmatite), open square - lilac lepidolite (E pegmatite), black filled square - pseudomorphic Cs-lepidolite (E pegmatite).

The primary fractionation of Nb-tantalates is distinct in both pegmatites. Disequilibrium phenomena of primary columbites - tantalites causes convolute oscillatory zoning observed in the periphery of the crystals, but the mobility of Nb and Ta are minor.

Some uranomicrolite forms at the lowest temperature in paragenesis with U-rich zircon. The deposition of P-rich zircon may be concomitant with secondary phosphates. Paragenetic relations and mineral-chemical fractionation trends of some indicative phases suggests that the hydrothermal evolution mobilises F in the earlier post-magmatic stages.

The formation of tourmaline breccia by hydraulic fracturing in the E pegmatite (Fig. 1) is explained by the escape and transmission of residual differentiates in response to decompression and rupture of the magmatic chamber, producing miarolitic volumes where F-elbaites precipitated. In its origin should be considered a high volatile pressure and high exhumation rate or at greater depth, the influence of shear. Decompression in shear structures also facilitates the superimposed hydrothermal evolution.

REFERENCES

Baldwin, J., Hill, P.G., von Knorring, O., Oliver, G. 2000. Exotic aluminium phosphates, natromontebrasite, brazilianite, goyazite, gorceixite and crandallite from rare-element pegmatites in Namibia. *Mineralogical Magazine,* 64(6): 1147-1164.

Beurlen, H., Thomas, R., Barreto, S., Da Silva, M. 2003. Nova ocorrência de ferrowodginita em associação com cassiterite, struverite e tapiolite na Província Pegmatítica da Borborema, Nordeste do Brasil. *Estudos Geológicos,* 13:35-45.